

Sequence Learning using Equilibrium Propagation

Malyaban Bal, Abhroni Sengupta

The Pennsylvania State University
mjb7906@psu.edu, sengupta@psu.edu

Abstract

Equilibrium Propagation (EP) is a powerful and more biologically plausible alternative to conventional learning frameworks such as backpropagation. The effectiveness of EP stems from the fact that it relies only on local computations and requires solely one kind of computational unit during both of its training phases, thereby enabling greater applicability in domains such as bio-inspired neuromorphic computing. The dynamics of the model in EP is governed by an energy function and the internal states of the model consequently converge to a steady state following the state transition rules defined by the same. However, by definition, EP requires the input to the model (a convergent RNN) to be static in both the phases of training. Thus it is not possible to design a model for sequence classification using EP with an LSTM or GRU like architecture. In this paper, we leverage recent developments in modern hopfield networks to further understand energy based models and develop solutions for complex sequence classification tasks using EP while satisfying its convergence criteria and maintaining its theoretical similarities with recurrent backpropagation. We explore the possibility of integrating modern hopfield networks as an attention mechanism with convergent RNN models used in EP, thereby extending its applicability for the first time on two different sequence classification tasks in natural language processing viz. sentiment analysis (IMDB dataset) and natural language inference (SNLI dataset).

Introduction

Equilibrium Propagation (EP) (Scellier and Bengio 2017) is a biologically plausible learning algorithm to train artificial neural networks. It requires only one computational circuit and single type of network unit during the two phases of training, whereas backpropagation requires a specialised type of computation during the backward phase to explicitly propagate errors which is different from the computational circuitry needed during the forward phase, thus it is essentially considered to be biologically implausible (Crick 1989). In EP, errors are propagated implicitly in the energy based model through local perturbations being generated at the output layer, unlike in backpropagation. Moreover, strong theoretical connections (Scellier and Bengio 2019) between EP and recurrent backpropagation (Almeida 1990; Pineda 1987) as well as the former's similarity regarding weight updates with spike-timing dependent plasticity (Bi and Poo 1998; Scellier and Bengio 2017) (a feasible model

to understand synaptic plasticity change in neurons) makes EP an interesting foundation to further understand biological learning (Lillicrap et al. 2020). Intrinsic properties of EP also provides the opportunity to design energy efficient implementations of the former on hardware unlike backpropagation through time (Martin et al. 2021).

The idea that neurons collectively adjust themselves to configurations according to the sensory input being fed into a neural network system such that they can better predict or explain the input data has been a quite popular hypothesis (Hinton 2002; Berkes et al. 2011). The collective neuron states can be interpreted as explanations of the input data. EP also consists of this central idea where the network, which is essentially a dynamical system following certain dynamics, converges to lower energy states which better explains the static input data.

In this paper, we have primarily discussed EP in a discrete time setting and used the scalar primitive function ϕ (Ernoult et al. 2019; Laborie et al. 2021) to derive the transition dynamics instead of an energy function as used in the initial works (Scellier and Bengio 2017). Primarily algorithms using EP have been designed for convergent RNNs (Laborie et al. 2021) which are neural networks that take in a static input and through the recurrent dynamics (as governed by the transition function – scalar primitive function of the system in our case) converges to a steady state which denotes the prediction of the network for that input. Training using EP primarily comprises of two distinct phases. During the first phase i.e. the “free” phase, the network converges to a steady state following only the internal dynamics of the system. In contrast, in the second phase the output layer (which acts as the prediction after the “free” phase has converged) is “nudged” closer to the actual ground truth and the local perturbations resulting from that change propagates to the other layers of the convergent RNN, forming local error signals in time which matches the error propagation associated with backpropagation through time (Ernoult et al. 2019). The state updates and the consequent weight updates of the system can be done through local in space computations. Moreover, further development in the topic has resulted in a modified method of weight update which is local in time as well (Ernoult et al. 2019), thus making learning algorithms using EP highly suitable for developing low-powered energy efficient neuromorphic implemen-

tations (Martin et al. 2021).

Till now, EP has been confined in the domain of image classification, the primary reason being the constraint associated with convergent RNNs which requires the input to be static. Developing an LSTM like architecture which is fed with a time-varying sequence of data instead of static data is not possible maintaining the constraints of EP. Results obtained for tasks such as sentiment analysis or inference problems by simply feeding the entire input sequence as input also results in poor solutions since the dependencies between the different parts of the sequence cannot be captured in that technique. However, with recent developments in the domain of modern dense hopfield networks, we have the ability to extend the capability of algorithms using EP to perform efficient sequence classification.

Hopfield networks were one of the earliest energy based models which were based on convergence to a steady state by minimizing an energy function which is an intrinsic attribute of the system. Hopfield networks were primarily used as associative memory, where we can store and retrieve patterns (Hopfield 1982). Classical hopfield networks were designed for storage and retrieval of binary patterns and the capacity of storage was limited since the energy function used was quadratic in nature. However, modern hopfield networks (Krotov and Hopfield 2016, 2018; Ramsauer et al. 2020) follow an exponential energy function for their internal state transitions which offers the possibility to store exponential number of continuous patterns and allows for faster single step convergence (Demircigil et al. 2017) during retrieval. Modern hopfield layer has been used previously for sequence-attention in conventional deep learning models with backpropagation as the learning framework (Widrich et al. 2020). In this paper, we integrate the capability of modern hopfield networks as a transformer-like (Vaswani et al. 2017) attention mechanism inside a convergent RNN and consequently train the resulting model using the learning rules defined by EP.

Modern hopfield networks fit perfectly in the context of convergent RNNs since both of them can be treated as energy-based models which are governed by their respective state transition dynamics. In a discrete time setting - which is primarily discussed in this paper - both of them follow a certain state transition rule at every time step which is governed by their defining energy function or a scalar primitive function in case of a convergent RNN. As we will see in later sections, the one step convergence guarantee of modern hopfield networks allows us to seamlessly interface it with a convergent RNN allowing both the networks to settle to their respective equilibrium states as the system converges as a whole. The fact that the convergent RNN converges to a steady state during both the “free” and “nudge” phases of its training process even after integrating the state transitions associated with the modern hopfield layer helps to maintain its theoretical connections with recurrent backpropagation.

The primary contributions of our paper are as follows:

- We explore for the first time how modern hopfield networks can fit into the setting of a convergent RNN model and how we can leverage the attention mechanism of the former to solve complex sequence classification prob-

lems using EP.

- We illustrate how to combine the state transition dynamics of both the hopfield network and underlying convergent RNN to converge to steady states during the “free” phase and the “nudge” phase of EP thus maintaining the latter’s theoretical equivalence with recurrent backpropagation w.r.t. gradient estimation.
- We report for the first time the performance of EP as a learning framework on widely known natural language processing tasks such as sentiment analysis (IMDB dataset) and natural language inference problems (Stanford Natural Language Inference - SNLI dataset) and compare the results with state-of-the-art architectures developed with an LSTM or GRU like framework and trained using backpropagation.

Background

In this section, we will discuss the workings of EP and its theoretical connections with backpropagation through time. We will then delve into the details of the modern hopfield layer which supports continuous patterns and will discuss the state transitions associated with it. We will further investigate the metastable states that arises in modern hopfield networks and will discuss how we can leverage them to form efficient encoding of the input sequences for our sequence classification problems.

Equilibrium Propagation

EP applies to convergent RNNs whose input at each time step is static and the state of the network eventually settles to a steady-state following a state update rule that is derived from the scalar primitive function ϕ . Moreover, the weights defined between two layers are symmetric in nature i.e. if the weight between layers s^i and s^{i+1} is w_i , then the weight of the connection between s^{i+1} and s^i is w_i^T . The state transition is defined as,

$$s_{t+1} = \frac{\partial \phi}{\partial s}(x, s_t, \theta) \quad (1)$$

where, $s_t = (s_t^1, s_t^2, \dots, s_t^n)$ is the collective state of the convergent RNN with n layers at time t , x is the input to the convergent RNN and θ represent the network parameters i.e. it comprises of the weights of each of the connections between layers. We do not consider any skip connection or self-connection in the convergent RNNs discussed but there has been some work done in that area (Gammell et al. 2021). The state transitions result in a final convergence to a steady state s_* after time T , such that $s_t = s_* \forall t \geq T$ and it satisfies the following condition,

$$s_* = \frac{\partial \phi}{\partial s}(x, s_*, \theta) \quad (2)$$

Training of convergent RNNs using EP comprises mainly of two different phases. However, an advanced variant with three phases (Laborieux et al. 2021) has been discussed later. During the first phase or the “free” phase the RNN follows the transition function as mentioned in Eqn. 1 and eventually reaches the steady state defined as the free fixed point

s_* after T time steps. We use the output layer of the steady state s_* i.e. s_*^n to make the prediction for the current input x . In the second phase or the “nudge” phase, an additional term $-\beta \frac{\partial L}{\partial s}$ is added to the state dynamics which immediately results in the state of the output layer being slightly nudged in the direction to minimize the loss function L (as defined between the target y and the output of the last layer of the convergent RNN). Though the internal states of the hidden layers are initially at the free fixed point state, they are eventually nudged to a different fixed point - weakly clamped fixed point s_*^β - because of the perturbations initially originated at the output layer. β is a small scaling factor defined as the “influence parameter” or “clamping factor” (Scellier and Bengio 2017) i.e. it controls the influence of the loss on the actual primitive scalar function during the second phase.

Thus initial state of the second phase is $s_0^\beta = s_*$ and the transition function is defined as,

$$s_{t+1}^\beta = \frac{\partial \phi}{\partial s}(x, s_t^\beta, \theta) - \beta \frac{\partial L}{\partial s}(s_t^\beta, y) \quad (3)$$

Following Eqn. 3, the convergent RNN settles to the steady state s_*^β after K timesteps. After the two phases are done, the learning rule to update the model parameters in order to minimize the loss $L^* = L(s_*, y)$ is defined as, $\Delta\theta = \eta \nabla_\theta^{EP}(\beta)$, (Scellier and Bengio 2017) where η is the learning rate and $\nabla_\theta^{EP}(\beta)$ can be defined as,

$$\nabla_\theta^{EP}(\beta) = \frac{1}{\beta} \left(\frac{\partial \phi}{\partial \theta}(x, s_*^\beta, \theta) - \frac{\partial \phi}{\partial \theta}(x, s_*, \theta) \right) \quad (4)$$

The defined convergent RNN can also be trained by back-propagation through time (BPTT) (Laborieux et al. 2021). According to the property of Gradient-Descent Updates (GDU) (Ernoult et al. 2019), the gradient updates computed by the EP algorithm is approximately equal to the gradient computed by BPTT ($\nabla^{BPTT}(t)$), according to relative mean squared error metric (RMSE), provided the convergent RNN has reached its steady state in $T - K$ steps during the first phase and $\beta \rightarrow 0$. Thus for initial K steps of the “nudge” phase we can state, $\forall t = 1, 2, \dots, K$

$$\nabla_\theta^{EP}(t, \beta) = \frac{1}{\beta} \left(\frac{\partial \phi}{\partial \theta}(x, s_t^\beta, \theta) - \frac{\partial \phi}{\partial \theta}(x, s_*, \theta) \right) \quad (5)$$

$$\nabla_\theta^{EP}(t, \beta) \xrightarrow{\beta \rightarrow 0} \nabla^{BPTT}(t) \quad (6)$$

In the traditional implementations of EP, two phases are involved, one with $\beta = 0$ i.e. the “free” phase and the other with $\beta > 0$ i.e. the “nudge” phase. In order to circumnavigate the first order bias that is induced into the system by assuming $\beta > 0$, a new implementation of EP was proposed (Laborieux et al. 2021) which comprises of a second “nudge” phase with $-\beta$ as the influence factor. Thus the algorithm comprises of three phases. The symmetric EP gradient estimates are thus free from first order bias and are more close to that of the values computed using BPTT and is defined as,

$$\nabla_\theta^{EPsym}(\beta) = \frac{1}{2\beta} \left(\frac{\partial \phi}{\partial \theta}(x, s_*^\beta, \theta) - \frac{\partial \phi}{\partial \theta}(x, s_*^{-\beta}, \theta) \right) \quad (7)$$

Modern Hopfield Network

The recent developments in modern hopfield networks (Ramsauer et al. 2020) offers exponential storage capacity and one step retrieval of stored continuous patterns. The increased storage capacity and the attention-like state update rule of modern hopfield layers can be leveraged to retrieve complex representation of the stored patterns which consists of richer embedding similar to that of attention mechanism inside transformers. In order to allow for continuous states, the energy function of the modern hopfield network is modified accordingly (Widrich et al. 2020), and it can be represented as,

$$E = -lse(\beta, X^T \xi) + \frac{1}{2}(\xi^T \xi) + \beta^{-1} \log N + \frac{1}{2} M^2 \quad (8)$$

$$lse(\beta, x) = \beta^{-1} \log \left(\sum_{i=1}^N \exp(\beta x_i) \right)$$

where, $X = (x_1, x_2, \dots, x_N)$ are N continuous stored patterns, ξ is the state pattern, M is the largest norm of all the stored patterns and $\beta > 0$. In general, the energy function of modern hopfield networks can be defined as, $E = -\sum_{i=1}^N F(x_i^T \xi)$ (Kroto and Hopfield 2016). For example, if we use the function $F(x) = x^2$, we describe the classical hopfield network which had limitations in storage capacity and also supported only binary patterns. However, with the introduction of an exponential interaction function like log-sum-exponential (lse) function, the storage capacity can be increased exponentially while enabling continuous patterns to be stored. Using Concave-Convex-Procedure (CCCP) (Yuille and Rangarajan 2001, 2003), the state update rule for the modern hopfield network (Ramsauer et al. 2020) can be defined as,

$$\xi^{new} = X \text{softmax}(\beta X^T \xi) \quad (9)$$

where, ξ^{new} is the retrieved pattern from the hopfield network.

We can define Query ($Q = RW_Q$) as ξ^T and Key ($K = YW_K$) as X^T . Thus the new form can be represented as,

$$Q^{new} = \text{softmax} \left(\frac{1}{\sqrt{d_k}} RW_Q W_K^T Y^T \right) Y W_K \quad (10)$$

$$Q^{new} = \text{softmax} \left(\frac{1}{\sqrt{d_k}} Q K^T \right) K$$

where, d_k is the encoding dimension of Key (K). The above representation (Ramsauer et al. 2020) is to emphasise on the similarity of the update rule of modern hopfield networks and the attention mechanism in transformers involving Query-Key pairs. Q represents the state pattern whereas Q^{new} represents the state pattern retrieved after the state transition. The linear projection matrices are defined as, $W_Q \in \mathbb{R}^{d_r \times d_k}$ and $W_K \in \mathbb{R}^{d_y \times d_k}$. There is theoretical guarantee that the modern hopfield network converges to a steady state (with exponentially small separation) after a single update step (Ramsauer et al. 2020) and therefore we successfully navigate to a fixed point at every time step. We can project the Q^{new} through $W_V \in \mathbb{R}^{d_k \times d_v}$ to generate a final output. The hopfield attention mechanism thus provides a rich representation of the stored patterns which helps in the case of sequence classification.

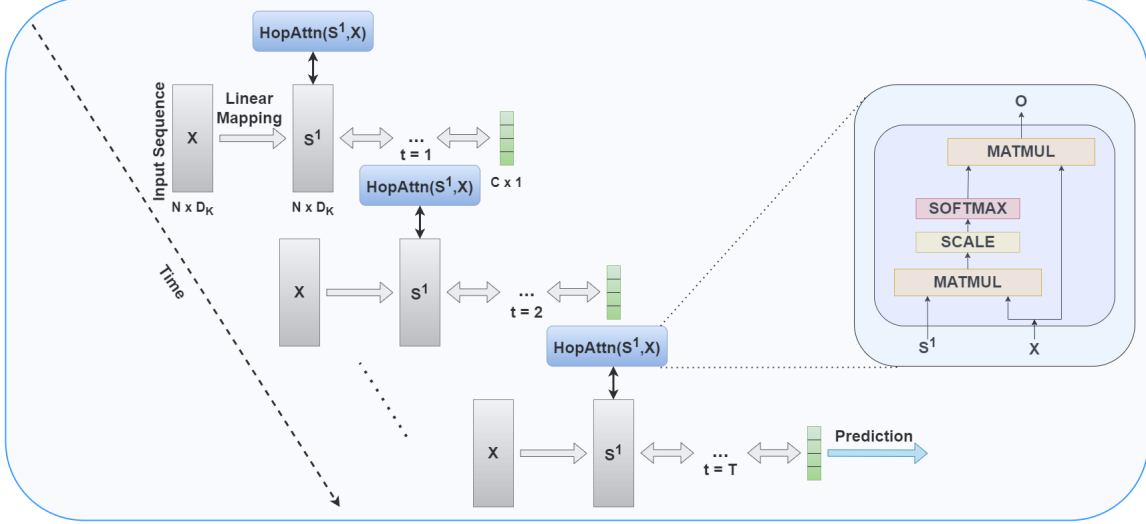


Figure 1: Simplistic scenario of application of $HopAttn$ modules in convergent RNN for a sequence classification problem with c classes has been described. The input X is directly fed as the Key K to the $HopAttn$ module. During the “free” phase (as described here), the model evolves through time following the defined state transition dynamics and converges to a steady state configuration after T time steps to settle to the prediction. The operations inside the $HopAttn$ module are also illustrated in details.

Metastable States in Hopfield Networks

The factor β , as defined in Eqn. 9, plays an important role in establishing the fixed points in the modern hopfield network (Ramsauer et al. 2020). The retrieved state pattern (or Q^{new} as defined above) settles to the defined fixed points following the state transition rule (Eqn. 10). However, if β is very high and/or the stored patterns are well separated, then we can easily retrieve the actual pattern stored in the hopfield networks. On the other hand, if β is low and the stored patterns are not all well separated but forms cluster like structures in the encoding dimension of the patterns, then the hopfield network generates metastable states. Thus, when we try to retrieve using a particular state pattern, we might converge to a metastable point which comprises of a richer representation of a number of patterns in that region. For incorporating such attention like behavior, we need to keep β small and usually $\beta = 1/\sqrt{d_k}$, where d_k is the encoding dimension of the stored patterns.

Proposed Methodology

We propose a novel methodology that harnesses the power of modern hopfield networks and allows us to seamlessly interface it with convergent RNNs, thus allowing sequence classification using EP. The input to the model is the sequence of patterns, $x \in R^{N \times D_K}$, where N is length of the sequence and D_K is the encoding dimension of the pattern. The state of the system at time t is defined as $s_t = (s_t^0, s_t^1, s_t^2, \dots, s_t^n)$, where n is the number of layers in the convergent RNN. The scalar primitive function (ϕ), which defines the state transition rules of the convergent RNN can

be defined as (Laborieux et al. 2021),

$$\phi(x, s, \theta) = s^{1T} \cdot w_1 \cdot x + \sum_{i=1}^{n-1} s^{i+1T} \cdot w_{i+1} \cdot s^i \quad (11)$$

where, w_{i+1} is the weight of the connection between s^i and s^{i+1} . x in later sections have been represented as s^0 . The list of weights is denoted by θ . The above scalar primitive function is primarily used when all the layers are fully connected, however a more specific ϕ as used in our work is described in details in Appendix: Algorithm.

Following the state transition as defined in Eqn. 10, the Hopfield Attention module can be defined as $HopAttn(Q, K)$, which has two critical inputs, viz. the Query (Q) which can be interpreted as the state pattern and the Key (K) which can be considered as the stored pattern. The dimension of the hopfield space is d_k . The underlying operations are illustrated in details in Fig. 1. The output of the $HopAttn$ function is defined as,

$$HopAttn(Q, K) = softmax\left(\frac{1}{\sqrt{d_k}} Q K^T\right) K \quad (12)$$

$HopAttn$ module plays a critical role in our convergent RNN by providing an attention based embedding of the input sequence resulting from their convergence to rich metastable states at every time step. In order to form the Query (Q) for the $HopAttn$ module, we define the layers connected to the input as projection layers (as demonstrated in Fig. 1) whose weight is analogous to W_Q . At every timestep t during the state transitions in the convergent RNN, the recurrent dynamics of the convergent RNN computes the Query (Q) to be fed to the $HopAttn$ module as illustrated in Eqn. 14. The stored sequence of patterns K is

fed directly into the *HopAttn* module. W_V is analogous to the weight of the output connection from the layer where *HopAttn* module is applied.

Transition Dynamics and Convergence

The state transition dynamics of the layers in the convergent RNN, except the last layer, where *HopAttn* is not applied is given by the following,

$$s_{t+1}^i = \sigma\left(\frac{\partial\phi}{\partial s^i}(x, s_t, \theta)\right) \quad (13)$$

where, σ is an activation function that restricts the range of the state variables to $[0, 1]$. However, for the layers where we apply the hopfield attention mechanism, the state transition function is updated as follows,

$$s_{t+1}^j = \text{HopAttn}\left(\frac{\partial\phi}{\partial s^j}(x, s_t, \theta), K\right) \quad (14)$$

where, s_{t+1}^j is the final state of the j^{th} layer (with *HopAttn* applied) at time $t+1$ and K is the sequence of stored patterns in the hopfield network which is usually the input x to the network.

Thus for the layers where we apply attention, we first follow the transition function of the underlying convergent RNN as defined by $\frac{\partial\phi}{\partial s^j}(x, s_t, \theta)$ and then we follow the update rule as derived from the modern dense hopfield network. Since convergence to a steady state is guaranteed after a single update step, there is no additional overhead for the hopfield network to converge and thus its state transition rule is only applied once.

The metastable states that the *HopAttn* module converges to after each timestep t eventually approaches steady state w.r.t the convergent RNN during both the phases of training of EP. The claim for such convergence can be further substantiated empirically by analysing the convergence of the dynamics of the model, governed by the scalar primitive ϕ with time. It is evident from Fig. 2b that even after we apply the *HopAttn* module (like in Fig. 1), the model still converges to a steady state eventually. Moreover, even after the integration of *HopAttn* modules, the GDU property of the convergent RNN still holds, thus maintaining the equivalence w.r.t gradient estimation of EP and BPTT (as described in Fig. 2a).

For the final layer, whose output is compared with the target label to calculate the loss function, the state update rule is defined as,

$$s_{t+1}^n = \sigma\left(\frac{\partial\phi}{\partial s^n}(x, s_t, \theta)\right) + \beta(y - s_t^n) \quad (15)$$

where, y is the target label and s_t^n is the output of the final layer at time t . $\beta = 0$ during the “free phase” and the loss function L used in this case is mean squared error.

Local Parameter Updates

The state update rule as defined above is essentially local in space since $\frac{\partial\phi}{\partial s^i}(x, s_t, \theta) \forall i = 1, \dots, n-1$ can be written as,

$$\frac{\partial\phi}{\partial s^i}(x, s_t, \theta) = w_i \cdot s_t^{i-1} + w_{i+1}^T \cdot s_t^{i+1} \quad (16)$$

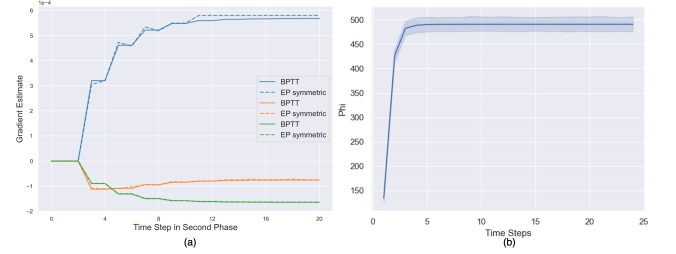


Figure 2: Results taken from experiments run on IMDB dataset. (a) Symmetric EP gradient estimate as defined in Eqn. 7 and gradient computed by BPTT, for three randomly chosen weights in the convergent RNN integrated with *HopAttn* module. (b) Convergence of the scalar primitive function ϕ with time upon using *HopAttn* in “free” phase taken over 50 phase transitions.

and for the final layer the same can be shown as,

$$\frac{\partial\phi}{\partial s^n}(x, s_t, \theta) = w_n \cdot s_t^{n-1} \quad (17)$$

where all the associated parameters for the computation are locally connected in space and time. The computation required w.r.t the *HopAttn* module can also be done locally in space and time.

The parameter update rule of the network, as stated in the earlier section, is also local in space, i.e. we can compute the updated weights directly using the state of the connecting layers. In this paper, we have used the three phase EP and therefore we derive the weight update rule following Eqn. 7,

$$\Delta w_{i+1} = \frac{1}{2\beta} (s_*^{i+1, \beta} \cdot s_*^{i, \beta^T} - s_*^{i+1, -\beta} \cdot s_*^{i, -\beta^T}) \quad (18)$$

where, $s_*^{i, \beta}$ is the state of layer i after the first “nudge” phase with influence parameter β and $s_*^{i, -\beta}$ is the state of layer i after the second “nudge” phase with influence parameter $-\beta$.

The detailed final algorithm is added in Appendix: Algorithm in the technical appendix. It is further validated through the experiments reported in the next section that as we continue updating the states s_t (following the update rules governed by the primitive function (ϕ) and the energy function for the modern hopfield network), we reach steady states during both the “free” and “nudge” phases of EP. Thus, following the weight update procedure of EP, we can update the weights through local in space update rules which enables us to develop state-of-the-art architectures for sentiment analysis and inference problems - potentially implementable in energy efficient neuromorphic systems.

Experiments

In the experiments that are reported in this section, we focus more on benchmarking with models that are trained using backpropagation such as LSTMs, GRUs, LMUs etc. since this is the first work to report the performance of convergent RNNs that are trained using EP on the specified datasets

for the task of sequence classification. In the following subsections, we define specific architectures for different sub-tasks in natural language processing. For testing our proposed work on sentiment analysis problems we chose the IMDB Dataset and for natural language inference problems, we chose the Stanford Natural Language Inference (SNLI) dataset. Further details regarding hyperparameters, coding platform and hardware used for training have been added to Appendix: Experimental Details in the technical appendix.

Sentiment Analysis

We have used IMDB dataset (Maas et al. 2011) to demonstrate the application of our model on sentiment analysis tasks. IMDB dataset comprises of 50K reviews, 25K for training and 25K for testing. Each of the reviews are either classified as positive or negative. The pre-processed IMDB dataset, available in Keras, is used in our experiments.

Architecture: 300D word2vec embeddings (Mikolov et al. 2013) are used for generating the word embeddings that are then fed into the convergent RNN and the maximum sequence length is restricted to 600. We have a single attention module applied to the first layer similar to Fig. 1. The hopfield layer provides a richer representation of the input sequence - encoding the dependencies between different components of the input sequence just like attention mechanism. The convergent RNN used for this experiment comprises of two fully connected hidden layers on top of the first projection layer. Modified EP is used for learning which comprises of three phases and removes first order bias, as described in the earlier section.

Model	Method	Accuracy
Simple Conv RNN	EqProp	79.8
ReLU GRU	BackProp	84.8
GRU	BackProp	86.5
Skip GRU	BackProp	86.6
Skip LSTM	BackProp	87.0
LSTM	BackProp	87.2
CoRNN	BackProp	87.4
UniCORNN	BackProp	88.4
Our Model	EqProp	88.96

Table 1: Result obtained from our model trained with EP compared with other models trained using backpropagation on the IMDB dataset.

Results: The results obtained by our model are compared with other models that can be potentially implemented in a neuromorphic system. However, all the other models are trained using backpropagation. Moreover, since we have not used a sophisticated language model that uses context to generate word embeddings, we are not comparing our results with state-of-the-art Transformers. The proposed model is compared with the best documented results of ReLU GRU (Dey and Salem 2017), GRU (Campos et al. 2017), Skip GRU (Campos et al. 2017), LSTM (Campos et al. 2017), Skip LSTM (Campos et al. 2017), CoRNN (Rusch and Mishra 2020), UniCORNN (Rusch and Mishra 2021). The

results from our model are the first to report performance on any sentiment analysis task using EP as a learning framework.

In order to stress on the advantage of using modern hopfield networks as an attention mechanism, we compare the accuracy achieved using our model against a vanilla implementation of EP on a convergent RNN with same depth but without any *HopAttn* modules and we see that our proposed model outperforms with a big margin ($> 9\%$). The case where hopfield attention modules were not used seems to converge early during training, thereby resulting in overfitting. However, as is evident from Fig. 3, usage of modern hopfield networks results in better generalization.

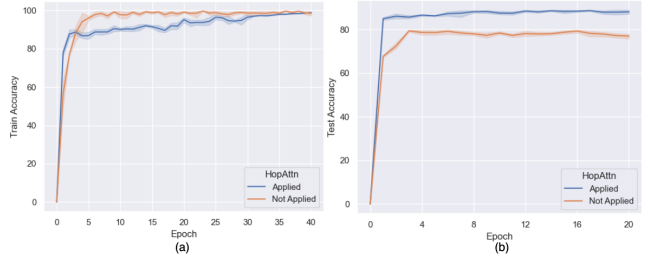


Figure 3: (a) Train Accuracy and (b) Test Accuracy comparison of two different convergent RNN models trained with EP - one with a *HopAttn* module applied (as shown in Fig. 1) and one without it. Results are taken over 5 different runs.

Natural Language Inference Problems

We have used Stanford Natural Language Inference (SNLI) (Bowman et al. 2015) dataset to demonstrate the application of our model on natural language inference (NLI) tasks. NLI generally deals with the classification of a pair of sentences namely, a premise and a hypothesis. A model, when given both the sentences as inputs, is able to predict whether the relationship between the two sentences signify an entailment, contradiction or if they are neutral. SNLI dataset comprises of 570K pairs of premises and hypotheses. For the task of classification, we remove the sentences which are unlabeled i.e. those that do not have a gold label and thus we have 549K pairs for training, 9842 for test and 9842 for validation. As specified earlier, there are three kinds of labels viz. entailment, contradiction and neutral.

Architecture: The premise and the hypothesis are encoded as a sequence of 300D word2vec word embeddings (Mikolov et al. 2013). The hopfield attention modules are used as specified in the Fig. 4. The architecture defined for this problem is inspired from the decomposable attention model (Parikh et al. 2016). Let us denote the premise as $A = (a_1, a_2, \dots, a_m)$ and hypothesis as $B = (b_1, b_2, \dots, b_n)$, where $a_i, b_j \in R^d$, d is the dimensionality of the word vector and m and n are the length of the sequences of the premise and hypothesis. We compute the new vectors $A' = HopAttn(s^{11}, A)$ and $B' = HopAttn(s^{14}, B)$, where s^{11} and s^{14} are values of the layers as shown in Fig. 4. These two vectors represent self-attention within A and B respec-

tively. Moreover, we also compute two other vectors, $\alpha = \text{HopAttn}(s^{13}, A)$ which represents the soft alignment of premise with the hypothesis B and $\beta = \text{HopAttn}(s^{12}, B)$ which represents the soft alignment of hypothesis with the premise A , where s^{13} and s^{12} are values of the layers as shown in Fig. 4. We then concatenate all the sequences and feed them to the next layer of the convergent RNN as demonstrated in Fig. 4. Modified three-phased EP is used for learning which reduces first order bias thereby providing better gradient estimates for weight update. For each of the sentences in both premise and hypothesis, we restrict the maximum sequence length to 25.

Model	Method	Accuracy
100D LSTM encoders	BackProp	77.6
Lexicalized Classifier	BackProp	78.2
Parallel LMU	BackProp	78.8
300D LSTM RNN encoders	BackProp	80.6
DELTA - LSTM	BackProp	80.7
300D SPINN-PI-NT	BackProp	80.9
Our Model	EqProp	81.45

Table 2: Result obtained from our model trained with EP compared with other models trained with backpropagation on SNLI dataset.

Results: The results obtained by our model are compared with other models trained using backpropagation reported in literature that can be potentially implemented in a neuromorphic setting. Like before, since we did not use a sophisticated pretrained language model that uses context to generate word embeddings, we are not comparing our results with state-of-the-art Transformers. The proposed model is compared with Lexicalized Classifier (Bowman et al. 2015), 100D LSTM encoders (Bowman et al. 2015), 300D LSTM RNN encoders (Bowman et al. 2016), 300D SPINN-PI-NT (Bowman et al. 2016), DELTA LSTM (Han et al. 2019), Parallel LMU (Chilkuri and Eliasmith 2021). The results from our model are the first to report performance on any NLI task using EP as a learning framework. The architecture proposed is just one of the possible variants, multiple other ways of applying *HopAttn* module can be explored for this dataset which might result in even better accuracies.

Discussion

The ability to think of neural networks as a dynamical system helps to further deepen our understanding regarding learning frameworks and intrigues us to delve deeper into the learning processes inside the brain. The bio-plausible local learning framework that EP provides can be best utilised in a neuromorphic system. An energy efficient, low powered neuromorphic implementation of the proposed sequence learning network trained using EP can be used in various real-time scenarios such as intrusion detection, real-time natural language processing, etc.

In this paper, we explore the application of EP as a learning framework in convergent RNNs integrated with mod-

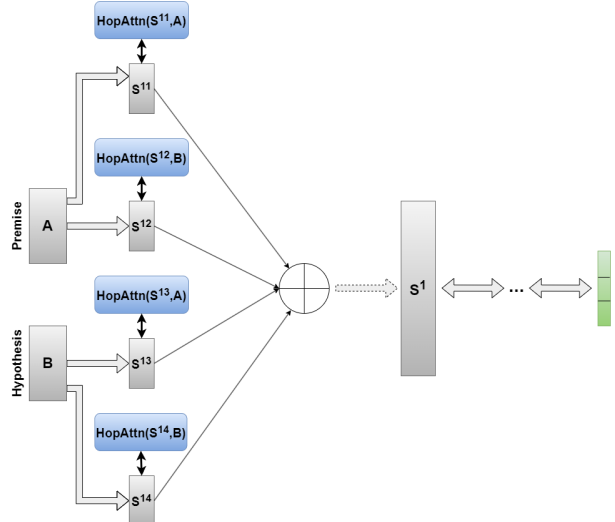


Figure 4: High-level overview of the architecture used in case of NLI problems (SNLI dataset). *HopAttn* modules are used in-order to generate embeddings comprising of dependencies inside different parts of a sentence as well as cross-attention between two different sentences and then the output of each of the layers are concatenated. The above described convergent RNN also converges over time during both the “free” and “nudge” phases of EP.

ern hopfield networks to solve sequence classification problems. We report for the first time the performance of EP on datasets such as IMDB and SNLI. The seamless use of hopfield attention modules helps in converging to better predictions that are not possible using a simple vanilla convergent RNN. Moreover, the constraint of EP requiring static input to the convergent RNNs makes it really difficult to train on datasets with sequence of data, thus an attention-like-mechanism provided by modern hopfield networks is ideal to encode the long-term dependencies in the sequence. The spatially (and potentially temporal) local weight update feature of EP still holds even after introducing the modern hopfield networks and therefore it can be easily converted into a neuromorphic implementation following the works of (Martin et al. 2021).

Implementing the methodology described in this paper in a neuromorphic setting can be a follow up task which will truly benefit from the single circuit and local in nature computation of EP. Certain unexplored areas in the paper can be future scope of the research. Firstly, due to limitations of EP it was not possible to use sophisticated context-aware language models for word embeddings, thus circumnavigating that challenge to achieve even better accuracy can be an interesting problem. Secondly, another intrinsic restriction of the convergent RNN model used in the experiments is that the weights of the connections needs to be symmetric. In order to make the model more bio-plausible with asymmetric connections, Vector Field method as proposed by (Scellier et al. 2018) can be further explored. Finally, although storing small sequence lengths like that of SNLI is not a big

concern, the memory overhead increases with increased sequence sizes like that of IMDB dataset. Thus a future endeavor can be made to solve it by redesigning EP or the convergent RNN such that it supports time-varying inputs and not just static input data.

References

Almeida, L. B. 1990. A learning rule for asynchronous perceptrons with feedback in a combinatorial environment. In *Artificial neural networks: concept learning*, 102–111.

Berkes, P.; Orbán, G.; Lengyel, M.; and Fiser, J. 2011. Spontaneous cortical activity reveals hallmarks of an optimal internal model of the environment. *Science*, 331(6013): 83–87.

Bi, G.-q.; and Poo, M.-m. 1998. Synaptic modifications in cultured hippocampal neurons: dependence on spike timing, synaptic strength, and postsynaptic cell type. *Journal of neuroscience*, 18(24): 10464–10472.

Bowman, S. R.; Angeli, G.; Potts, C.; and Manning, C. D. 2015. A large annotated corpus for learning natural language inference. *arXiv preprint arXiv:1508.05326*.

Bowman, S. R.; Gauthier, J.; Rastogi, A.; Gupta, R.; Manning, C. D.; and Potts, C. 2016. A fast unified model for parsing and sentence understanding. *arXiv preprint arXiv:1603.06021*.

Campos, V.; Jou, B.; Giró-i Nieto, X.; Torres, J.; and Chang, S.-F. 2017. Skip rnn: Learning to skip state updates in recurrent neural networks. *arXiv preprint arXiv:1708.06834*.

Chilkuri, N. R.; and Eliasmith, C. 2021. Parallelizing legendre memory unit training. In *International Conference on Machine Learning*, 1898–1907. PMLR.

Crick, F. 1989. The recent excitement about neural networks. *Nature*, 337(6203): 129–132.

Demircigil, M.; Heusel, J.; Löwe, M.; Uppgang, S.; and Vermet, F. 2017. On a model of associative memory with huge storage capacity. *Journal of Statistical Physics*, 168(2): 288–299.

Dey, R.; and Salem, F. M. 2017. Gate-variants of gated recurrent unit (GRU) neural networks. In *2017 IEEE 60th international midwest symposium on circuits and systems (MWSCAS)*, 1597–1600. IEEE.

Ernoult, M.; Grollier, J.; Querlioz, D.; Bengio, Y.; and Scellier, B. 2019. Updates of equilibrium prop match gradients of backprop through time in an RNN with static input. *Advances in neural information processing systems*, 32.

Gammell, J.; Buckley, S.; Nam, S. W.; and McCaughan, A. N. 2021. Layer-Skipping Connections Improve the Effectiveness of Equilibrium Propagation on Layered Networks. *Frontiers in computational neuroscience*, 15: 627357.

Han, K.; Chen, J.; Zhang, H.; Xu, H.; Peng, Y.; Wang, Y.; Ding, N.; Deng, H.; Gao, Y.; Guo, T.; et al. 2019. Delta: A deep learning based language technology platform. *arXiv preprint arXiv:1908.01853*.

Hinton, G. E. 2002. Training products of experts by minimizing contrastive divergence. *Neural computation*, 14(8): 1771–1800.

Hopfield, J. J. 1982. Neural networks and physical systems with emergent collective computational abilities. *Proceedings of the national academy of sciences*, 79(8): 2554–2558.

Krotov, D.; and Hopfield, J. 2018. Dense associative memory is robust to adversarial inputs. *Neural computation*, 30(12): 3151–3167.

Krotov, D.; and Hopfield, J. J. 2016. Dense associative memory for pattern recognition. *Advances in neural information processing systems*, 29.

Laborieux, A.; Ernoult, M.; Scellier, B.; Bengio, Y.; Grollier, J.; and Querlioz, D. 2021. Scaling equilibrium propagation to deep convnets by drastically reducing its gradient estimator bias. *Frontiers in neuroscience*, 15: 129.

Lillicrap, T. P.; Santoro, A.; Marris, L.; Akerman, C. J.; and Hinton, G. 2020. Backpropagation and the brain. *Nature Reviews Neuroscience*, 21(6): 335–346.

Maas, A.; Daly, R. E.; Pham, P. T.; Huang, D.; Ng, A. Y.; and Potts, C. 2011. Learning word vectors for sentiment analysis. In *Proceedings of the 49th annual meeting of the association for computational linguistics: Human language technologies*, 142–150.

Martin, E.; Ernoult, M.; Laydevant, J.; Li, S.; Querlioz, D.; Petrisor, T.; and Grollier, J. 2021. Eqspike: spike-driven equilibrium propagation for neuromorphic implementations. *Iscience*, 24(3): 102222.

Mikolov, T.; Chen, K.; Corrado, G.; and Dean, J. 2013. Efficient estimation of word representations in vector space. *arXiv preprint arXiv:1301.3781*.

Parikh, A. P.; Täckström, O.; Das, D.; and Uszkoreit, J. 2016. A decomposable attention model for natural language inference. *arXiv preprint arXiv:1606.01933*.

Pineda, F. 1987. Generalization of back propagation to recurrent and higher order neural networks. In *Neural information processing systems*.

Ramsauer, H.; Schäfl, B.; Lehner, J.; Seidl, P.; Widrich, M.; Adler, T.; Gruber, L.; Holzleitner, M.; Pavlović, M.; Sandve, G. K.; et al. 2020. Hopfield networks is all you need. *arXiv preprint arXiv:2008.02217*.

Rusch, T. K.; and Mishra, S. 2020. Coupled Oscillatory Recurrent Neural Network (coRNN): An accurate and (gradient) stable architecture for learning long time dependencies. *arXiv preprint arXiv:2010.00951*.

Rusch, T. K.; and Mishra, S. 2021. UnICORNN: A recurrent model for learning very long time dependencies. In *International Conference on Machine Learning*, 9168–9178. PMLR.

Scellier, B.; and Bengio, Y. 2017. Equilibrium propagation: Bridging the gap between energy-based models and backpropagation. *Frontiers in computational neuroscience*, 11: 24.

Scellier, B.; and Bengio, Y. 2019. Equivalence of equilibrium propagation and recurrent backpropagation. *Neural computation*, 31(2): 312–329.

Scellier, B.; Goyal, A.; Binas, J.; Mesnard, T.; and Bengio, Y. 2018. Generalization of equilibrium propagation to vector field dynamics. *arXiv preprint arXiv:1808.04873*.

Vaswani, A.; Shazeer, N.; Parmar, N.; Uszkoreit, J.; Jones, L.; Gomez, A. N.; Kaiser, Ł.; and Polosukhin, I. 2017. Attention is all you need. *Advances in neural information processing systems*, 30.

Widrich, M.; Schäfl, B.; Pavlović, M.; Ramsauer, H.; Gruber, L.; Holzleitner, M.; Brandstetter, J.; Sandve, G. K.; Greiff, V.; Hochreiter, S.; et al. 2020. Modern hopfield networks and attention for immune repertoire classification. *Advances in Neural Information Processing Systems*, 33: 18832–18845.

Yuille, A. L.; and Rangarajan, A. 2001. The concave-convex procedure (CCCP). *Advances in neural information processing systems*, 14.

Yuille, A. L.; and Rangarajan, A. 2003. The concave-convex procedure. *Neural computation*, 15(4): 915–936.

Appendix: Algorithm

The scalar primitive function ϕ and the pseudocode for the algorithm designed to integrate modern hopfield networks into convergent RNNs and subsequently train the latter using the three phase (one free phase and two nudge phases) equilibrium propagation is described in this section.

Scalar Primitive Function ϕ

The scalar primitive function ϕ is used to derive the state transition dynamics of the convergent RNN. In the paper, a high level overview of the function ϕ is described where all the layers are fully connected. However in order to understand the sequence classification problems with inputs $x \in R^{N \times D_K}$, we need to further elaborate few underlying operations. If we consider the sentiment analysis problem with IMDB dataset, the first layer connected to the input is a linear projection layer, thus we can re-write the ϕ as,

$$\phi(x, s, \theta) = s^1 \bullet (x \cdot w_1) + s^{2T} \cdot w_2 \cdot F(s^1) + \sum_{i=2}^{n-1} s^{i+1T} \cdot w_{i+1} \cdot s^i \quad (19)$$

where \bullet represents euclidean scalar product of two tensors with same dimensions, $(x \cdot w_1)$ represents the linear projection of x through $w_1 \in R^{D_K \times D_K}$ and w_{i+1} is the weight of the connection between s^i and s^{i+1} . The flattened output of the first projection layer ($F(s^1)$ where F is the flattening operation from (A, B) to $(1, AB)$) is then fed into rest of the $n - 1$ fully connected layers. It must be noted that even if we use the first layer as a projection layer, the local state and weight update property is still preserved: $(\frac{\partial \phi}{\partial s^1}(x, s_t, \theta) = (x \cdot w_1) + F^{-1}(w_2^T \cdot s_t^2)$, where F^{-1} is inverse of F and $\Delta w_1 = \frac{1}{2\beta}(x^T \cdot s_*^{1,\beta} - x^T \cdot s_*^{1,-\beta})$. $\Delta w_{i+1} = \frac{1}{2\beta}(s_*^{i+1,\beta} \cdot s_*^{i,\beta T} - s_*^{i+1,-\beta} \cdot s_*^{i,-\beta T})$ is the general weight update rule for fully connected layers.

Pseudocode

Algorithm 1: (*stateUpdate*) The state update dynamics of the convergent RNN integrated with *HopAttn* module. Activation function σ removed for simplicity and we consider the input x as the stored patterns in the hopfield network.

Input: $x, y, s, \theta, \beta, T_\beta$
Parameter: Optional list of parameters
Output: s

- 1: $s_0 \leftarrow s$
- 2: **for** $t = 0$ to T_β **do**
- 3: **for** $i = 1$ to $n - 1$ **do**
- 4: $s_{t+1}^i \leftarrow \frac{\partial \phi}{\partial s^i}(x, s_t, \theta)$
- 5: **if** *isHopAttnApplied*(s_{t+1}^i) is True **then**
- 6: $s_{t+1}^i \leftarrow \text{HopAttn}(s_{t+1}^i, x)$
- 7: **end if**
- 8: **end for**
- 9: $s_{t+1}^n \leftarrow \frac{\partial \phi}{\partial s^n}(x, s_t, \theta) + \beta(y - s_t^n)$
- 10: **end for**
- 11: **return** s_{T_β}

Algorithm 2: Three-phase EP applied on the proposed convergent RNN model integrated with *HopAttn* layer.

Input: x, y, θ, η
Output: θ

- 1: $s_0 \leftarrow 0$
- 2: $s_T \leftarrow \text{stateUpdate}(x, y, s_0, \theta, 0, T)$
- 3: $s_* \leftarrow s_T$
- 4: $s_*^\beta \leftarrow \text{stateUpdate}(x, y, s_*, \theta, \beta, K)$
- 5: $s_*^{-\beta} \leftarrow \text{stateUpdate}(x, y, s_*, \theta, -\beta, K)$
- 6: $\nabla_\theta^{EPsym} \leftarrow \frac{1}{2\beta}(\frac{\partial \phi}{\partial \theta}(x, s_*^\beta, \theta) - \frac{\partial \phi}{\partial \theta}(x, s_*^{-\beta}, \theta))$
- 7: $\theta \leftarrow \theta + \eta \nabla_\theta^{EP}$
- 8: **return** θ

Appendix: Experimental Details

We implemented modified EP, as given by Algorithm 2, using PyTorch 1.7.0. The experiments were run on Nvidia GeForce RTX 2080 Ti GPUs (8). For each of the datasets used, the list of range of hyperparameters and their optimal values are given in the next section.

Sentiment Analysis (IMDB dataset)

In the sentiment analysis problems, we have 300D word2vec embeddings with maximum sequence length of 600 as the input to the convergent RNN. The first layer is a linear projection layer which maintains the same encoding dimension of 300. The hopfield attention module is integrated with the first layer. The final output of that layer is flattened and fed into a hidden layer of size 1000, followed by another layer of size 40 and then followed by the output layer of size 2. Adam optimizer is used as the optimizer to update the weights and the activation function is a modified form of hard sigmoid function. The loss function, as discussed in the paper, is mean squared error. GPU memory usage while training is limited to around 6.5GB with batch size of 100 and running time for one experiment is around 5 hours on the described hardware. The hyperparameters, GPU usage and time taken to achieve optimal accuracy is given in the table below,

Hyper-parameters	Optimal (Range Explored)
Influence Factor (β)	0.1 (0.05-0.8)
T (“Free Phase”)	50 (40-150)
K (“Nudge Phase”)	25 (15-80)
Max Epochs	50
Layer-wise Learning Rates	1e-4, 5e-5, 5e-5, 5e-5

Table 3: Hyper-parameters used for training our model on IMDB dataset.

Natural Language Inference (SNLI dataset)

We have 300D word2vec embeddings with maximum sequence length of 25 for both premise and hypothesis given as the input. The scalar primitive function can be considered to be of a similar form as given by Eqn. 19. However, we consider four linear projection layers connected to inputs A and

B , as depicted in the paper. Then the output of all the projection layers are concatenated and flattened to be fed into the remaining two fully connected layers. The architecture is kept simple to show the effectiveness of using the modern hopfield network. Activation function and optimizer used is the same as the previous experiment. GPU memory usage during training is limited to around 1.6 GB with batch size of 200. Running time for one experiment is around 6 hours. The hyperparameters and operational details are specified in Table 4.

Hyper-parameters	Optimal (Range Explored)
Influence Factor (β)	0.5 (0.1-0.8)
T (“Free Phase”)	60 (40-200)
K (“Nudge Phase”)	30 (15-100)
Max Epochs	50
Layer-wise Learning Rates	5e-4,5e-4,5e-4,5e-4,2e-4,2e-4

Table 4: Hyper-parameters used for training our model on SNLI dataset.

Implementation Details

In order to make the code simpler and intuitive, the automatic differentiation framework of PyTorch has been used in our code to calculate the state and weight update rules. The scalar primitive function ϕ has been defined for each of our test datasets according to the underlying architecture and then the state update dynamics and weight updates have been computed by taking the appropriate derivatives of ϕ . Such an implementation also makes the code robust to further changes in architecture.